ISSN 1882-3432

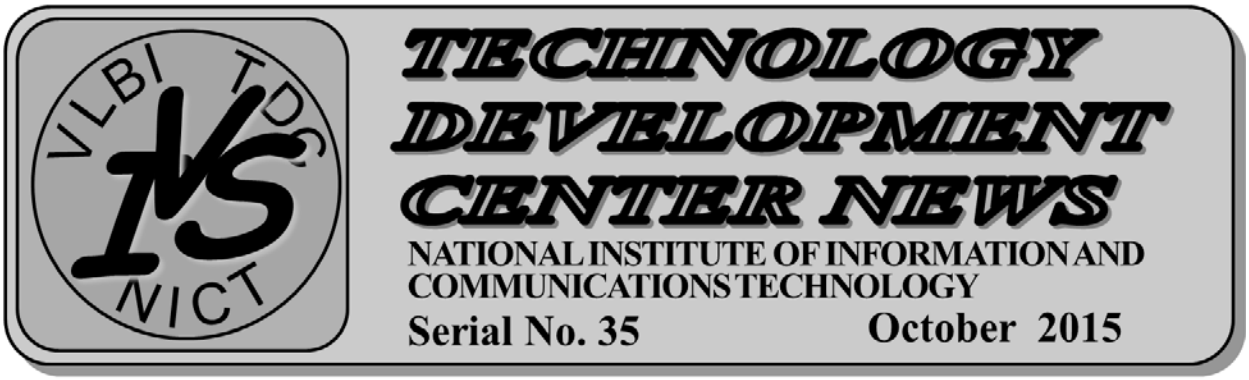

CONTENTS

Proceedings of the 14th NICT TDC Symposium (Kashima, 25 June, 2015)

First Geodetic Result of Ishioka VGOS Antenna

Yoshihiro Fukuzaki
(*fukuzaki-y96pe@mlit.go.jp*),
Kozin Wada, Ryoji Kawabata, Masayoshi Ishimoto, Takahiro Wakasugi

Geospatial Information Authority of Japan, Kitasato-1, Tsukuba, Ibaraki, Japan

Abstract: The Geospatial Information Authority of Japan (GSI) started a new project for constructing a VGOS station in Japan. The construction of the antenna (radio telescope) has been completed and the necessary equipment (Front-end, Back-end, H-maser, and so on) has also been delivered. The name of the new site is Ishioka, which is located 16.6 km away from Tsukuba 32-m antenna.

We briefly report the initial receiving performance of the Ishioka antenna, and the first geodetic result of VLBI observations carried out after February 2015.

1. Introduction

The Geospatial Information Authority of Japan (GSI) has carried out VLBI observations since 1981. In the first period from 1981 to 1994, we developed transportable VLBI systems with a 5-m antenna and a 2.4-m antenna and carried out domestic observations by using them. As a result, 8 sites in Japan were observed and precise positions determined. In addition, Japan-Korea VLBI observations were carried out by using a transportable 3.8-m antenna in 1995. In these observations, the Kashima 26-m antenna, which was removed in 2002, was used as a main station. Next, in the second period from 1994 to 1998, GSI established four permanent stations: Tsukuba 32-m, Shintotsukawa 3.8-m, Chichijima 10-m, and Aira 10-m antennas. Up to the present, regular VLBI observations by using the four stations have been carried out. Especially, Tsukuba 32-m antenna is a main station for not only domestic but also international VLBI observations now.

In 2011, GSI started a project for constructing a new antenna following the VLBI2010 concept, which is recommended by the International VLBI Service for Geodesy and Astrometry (IVS) as the next-generation VLBI system.

This paper gives the outline of the project, the initial receiving performance of the new antenna, and the first geodetic results of VLBI observations that have been carried out since February 2015.

2. Observing Facilities

In the new project, observing facilities are now being constructed. The conceptual design consisting of the six components is depicted in Figure 1. At present temporary operation rooms are installed instead of the Operation Building, and it will be completed by the end of February 2016.

The site name is Ishioka, which is located near Tsukuba (about 16.6 km-NE from Tsukuba 32-m antenna).

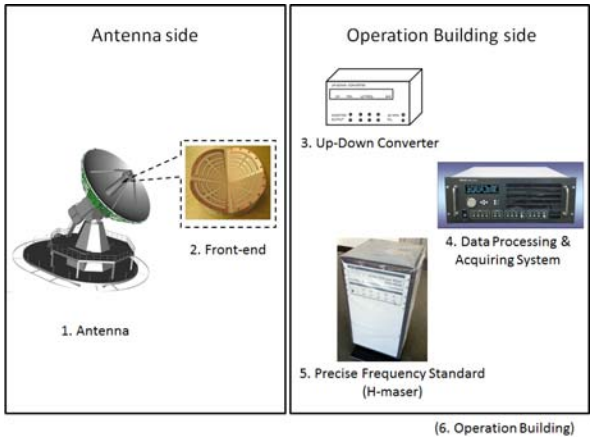

Figure 1. Conceptual design of the new observing facilities

3. Antenna and Front-end

3.1 Antenna

The antenna (radio telescope) is the main part of the observing system (Figure 2). Since a single antenna is employed, very high slew rates are specified in order to be compliant with the VLBI2010 concept. In addition, Ring Focus optics was applied for the antenna design in order to match the beam pattern of the broadband feed. The specifications of the antenna are listed in Table 1.

3.2 Front-end

According to the VLBI2010 concept, a broadband feed is necessary to achieve high aperture efficiency over 2–14 GHz. At present the Eleven feed, which has been developed at Chalmers University of Technology in Sweden, and Quadruple-Ridged Flared Horn (QRFH), which is developed at California Institute of Technology (Caltech), are the practical as a broadband feed, so both feed systems are purchased. The employment of the feed will be determined after the evaluation of the antenna receiving performance with these two feeds.

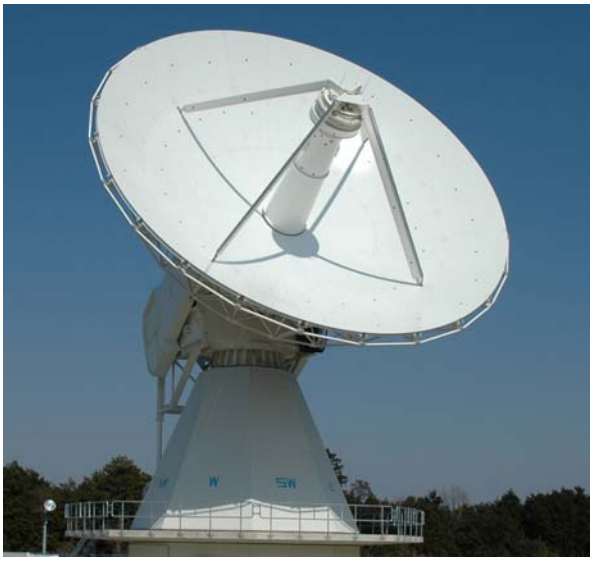

Figure 2. Photo of the new antenna.

Table 1. Specifications of the new antenna.

Parameter	Value
Diameter	13.2 m
RF frequency range	2–14 GHz
Optics	Ring Focus
Surface accuracy	$\leq$ 0.1 mm (rms)
AZ maximum slew rate	12°/sec
EL maximum slew rate	6°/sec
AZ maximum acceleration rate	3°/sec^2
EL maximum acceleration rate	3°/sec^2
Special feature	Reference point can be measured directly from the ground for co-location.

In the both cases, the feeds and Low Noise Amplifiers (LNAs) are integrated into the each cryogenic system, whose physical temperature is less than 20 K.

In addition, in order to achieve the compatibility with the legacy S/X band observation, tri-band feed system is also purchased. By using the tri-band feed system the measurement of the initial receiving performance was performed. (See the following section)

The phase and cable calibration system is also installed. A new type of P-cal unit, which was designed by Haystack observatory, is developed and employed. In addition, instead of the present D-cal unit a new cable calibration system developed by National Institute of Information and Communications Technology (NICT) is also employed. The specifications of the front-end are shown in Table 2.

Table 2. Specifications of the front-end.

Parameter	Value
RF frequency range	2–14 GHz
Polarization	Dual linear polarization
Feed	Eleven feed or QRFH
Dewar	Feed, LNAs, and other devices should be included and cooled by cryogenic system.
Physical temperature	$\leq$ 20 K
Receiver noise temperature	$\leq$ 30 K
Total gain	$\geq$ 45 dB
Output frequency range	2–14 GHz
Number of output	2 (for dual linear polarization)
Phase and delay calibration	New-type P-cal unit designed by Haystack Observatory New cable calibration system developed by NICT
Injection of P-cal/noise-source	pre-feed (Eleven feed) or pre-LNA (QRFH)

4. Receiving Performance

First of all, the receiving performance of the antenna with tri-band feed system was measured by receiving the radio signals from some strong radio stars (Cas-A, Taurus-A, Virgo-A). As a result, the SEFDs for X and S band are approximately 1,250 Jy and 1,700 Jy, respectively. This means that the aperture efficiencies for X and S band are 77% and 59%, respectively, if the system noise temperature is assumed as 50 K. High receiving performance for X band is confirmed as the feature of the Ring Focus optics. (The measurement of the receiving performance for Ka band is not done yet.)

As a next step QRFH system was installed on the antenna, and the receiving performance was measured. Unfortunately only the sun was detectable, and it was realized that the modification of the cryogenic dewar would be necessary to improve the

sensitivity of QRFH. We have a plan to improve the cryogenic dewar by the end of March 2016.

Finally, Eleven feed system was installed on the antenna, and the receiving performance was measured by receiving the radio signals from some strong radio stars (Cas-A, Taurus-A, Cygnus-A). The SEFD values in the frequency range from 3 to 14 GHz are shown in Figure 3. The SEFD values less than 9 GHz are acceptable (less than 2,000 Jy), but unfortunately the SEFD values more than 10 GHz are getting worse and reaching 7,500 Jy at 14 GHz.

On the other hand, RFI is more serious than expected because of the feature of Ring Focus optics. In the case of Ring Focus optics, the aperture efficiency is better but the artificial radio signal can reach the feed more easily than the usually-used optics like Cassegrain. In the new station, the RFI caused by the radio signal for cellular phone is so strong in the frequency range less than 2.1 GHz that the saturation of the amplifiers for S band occurs. In order to avoid the saturation of the S band amplifiers some filters (High Pass Filter (cut less than 2.2 GHz), Notch Filter (cut 2.1 GHz), and Band Pass Filter (pass 2.2-2.4 GHz)) are installed in the signal chain of the new antenna, and the VLBI observation can be carried out normally at present.

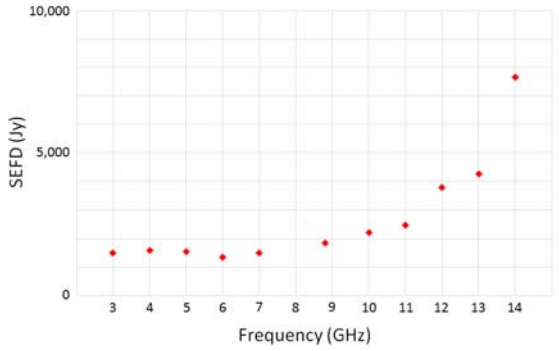

Figure 3. SEFD values of Ishioka VGOS antenna with Eleven feed

5. First Geodetic Result

First geodetic VLBI observation was carried out in February 2015 in the Japanese domestic network including GSI's VLBI stations (Tsukuba 32-m, Aira 10-m, and Chichijima 10-m antenna). Until the middle of June 2015 Ishioka station has participated in two types of VLBI sessions. One is Japanese domestic session JADE and the other is AOV (Asia-Oceania VLBI group for Geodesy and Astrometry) session, which newly started in 2015 for Asia-Oceania region. Totally ten 24-h VLBI sessions were observed at Ishioka station, and the precise geodetic results were successfully obtained for JADE sessions, which were analyzed by GSI quickly. The results of baseline lengths between Ishioka and Tsukuba 32-m antenna are listed in the Table 3. The standard deviation for each session is the range 1–2 mm, which is reasonable for Ishioka-Tsukuba baseline.

Table 3. Geodetic results of JADE sessions that were carried out at Ishioka station

Session	Date	Baseline Length
JD1502	Feb. 19	16,606,288.71 +- 1.58 mm
JD1503	Mar. 05	16,606,290.88 +- 1.04 mm
JD1504	Mar. 12	16,606,285.38 +- 1.39 mm
JD1505	Apr. 23	16,606,291.41 +- 1.31 mm
JD1506	May. 14	16,606,293.14 +- 1.50 mm
JD1507	Jun. 04	16,606,290.03 +- 1.27 mm
JD1508	Jun. 11	16,606,291.17 +- 1.34 mm

6. Summary

A new project for constructing a new antenna in Japan has started. The new station will be fully compliant with the VLBI2010 concept. The construction of the antenna was completed by the end of March 2014. The measurement of the receiving performance of the antenna was performed, and high aperture efficiency for X band was confirmed.

First geodetic VLBI observation was carried out in February 2015, and ten VLBI observations were performed till June 2015. As a result, precise coordinates of the new antenna were obtained successfully.

This station will play an important role as a main station in the Asian region instead of Tsukuba 32-m station in the near future.

7. Acknowledgments

VLBI operation software that is developed by National Aeronautics and Space Administration (NASA) is employed at Ishioka station. Installation and customization of this software were performed by NICT under the joint research agreement between GSI and NICT.

On a Wide-Band Bandwidth Synthesis II

Testuro Kondo (*kondo@nict.go.jp*)
and Kazuhiro Takefuji

Kashima Space Technology Center,
National Institute of Information and Communications Technology,
893-1 Hirai, Kashima, Ibaraki 314-8501, Japan

1. Introduction

A technique to carry out the bandwidth synthesis of wideband observation data exceeding a band width of 10 GHz has been developed. The technique excepting an ionospheric correction portion has been implemented in the bandwidth synthesizing software "KOMB" [*Kondo and Kunimori*, 1984; *Kondo et al.*, 1999]. The new KOMB has been successfully applied to process actual wideband VLBI data obtained on a short baseline of about 50km where an ionospheric effect can be neglected. As for the ionospheric correction, we have checked whether it worked well or not by using artificial correlation data simulating the effect of ionosphere. We also got a good result for the ionospheric correction.

2. Wide-band bandwidth synthesis (WBWS)

Two types of correction are considered in WBWS software. One is inter-band delay correction that is necessary to connect each band data in the frequency domain. System delay in a receiving system is usually different for each band. In order to connect different bands it is necessary to correct the system delay. The other is inner-band phase correction that increases a signal to noise ratio. Ionospheric correction is a kind of this correction, but it is handled separately and details are described later.

We have developed a realistic method to carry out the correction as follows. At first, we choose a scan which observes a strong radio source and define it as a "reference scan". Normal fringe search is carried out for each band data of the reference scan to obtain an observed delay for each band. We obtain the inter-band delay correction data (IDC) by differentiating each observed delays. The inner-band phase correction data (IPC) (may include the ionospheric effect at the reference scan) is obtained from the cross spectrum of each band after delay residual is corrected. The method is summarized as follows,

1) define a reference scan in an observation session,
2) do normal fringe search for each band in order to obtain delay residual $\Delta\tau_n$ where n is a band index and calculate cross spectrum after delay residual is corrected,
3) phase characteristics of cross spectrum obtained by step 2) is approximated by a 4th-order polynomial for each band, and they become IPC.
4) IDC is given by $\Delta\tau_n - \Delta\tau_1$, where $\Delta\tau_1$ is delay residual at band #1.
5) apply IDC and IPC obtained this way to raw correlation data not only for the reference scan but also for other scans, then carried out WBWS.

The ionospheric effect in the cross spectrum of the reference scan after the WBWS will not appear, because it is compensated by the IPC that already includes the ionospheric effect at the reference scan. However relative ionospheric effect can appear for a scan other than the reference scan. We can correct this ionospheric effect from the phase characteristics of cross spectrum as follows,

1) get group delays as a function of frequency (these are observed group delays) by calculating average phase gradient against frequency for each narrow frequency span from a cross spectrum after WBWS.
2) estimate $\Delta\tau_{ion}$ and ΔTEC from the observed group delays and a group delay model as follows:

$$\tau_g(f) = -\Delta\tau_{ion} + \alpha\Delta TEC f^{-2}$$

where α is a constant.

3) estimate only ϕ_c from the cross spectrum after WBWS and a phase model as follows:

$$\phi(f) = -2\pi f\Delta\tau_{ion} - 2\pi\alpha\Delta TEC f^{-1} + \phi_c$$

where $\Delta\tau_{ion}$ and ΔTEC are fixed to those estimated by step 2).

3. Results of WBWS

The KOMB implemented with a WBWS function is applied to wide-band VLBI data observed on the baseline between Kashima (NICT) station and Ishioka (GSI) station (about 50km length) (Fig.1) in January, 2015.

Fig.2 shows receiving frequency bands. Bands 1, 2, 3, and 4 are sampled by one sampler. Therefore

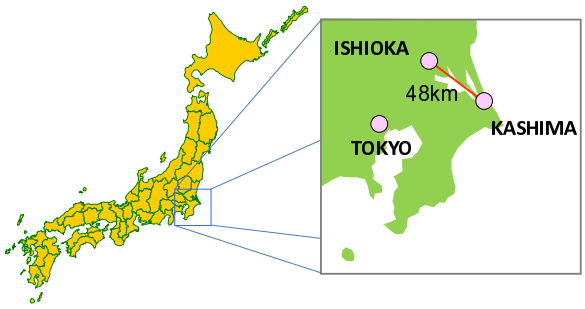

Figure 1. Location of Kashima-Ishioka baseline.

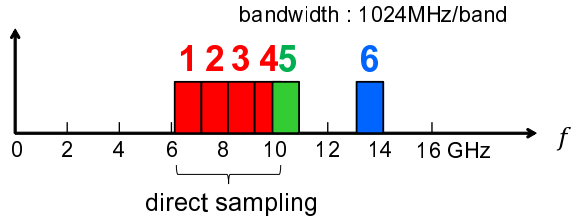

Figure 2. Receiving frequency bands. Bands 1, 2, 3, and 4 are sampled by one sampler. Bands 5 and 6 are sampled by different samplers. Each band width is 1024 MHz.

no system delay among bands appears, and we can assume these four bands as one single band spanning band 1 to 4. Bands 5 and 6 are sampled by different samplers.

Fig.3 shows a cross spectrum after WBWS processing for the reference scan. Note that phases are aligned in a line parallel to the frequency axis, and this means that WBWS is carried out successfully.

We have processed other scans by using the correction (IDC and IPC) obtained for the reference scan. Fig.4 shows an example of the results of other scan data. As shown in the figure, WBWS is also carried out successfully. As also shown in the figure, the ionospheric effect in the phase spectrum is not clear because of the shortness of a baseline length.

4. Evaluation of Ionospheric Correction

VLBI data observed on the Kashima-Ishioka baseline is not adequate to evaluate the ionospheric correction, because the baseline length is too short. Therefore VLBI data reflecting an ionospheric effect are generated from raw correlation data, and then the ionospheric correction is evaluated. Correlation data simulating the ionospheric effect being $R_i(\tau, k)$, where τ and k are a lag index and a time index, are generated from raw correlation data

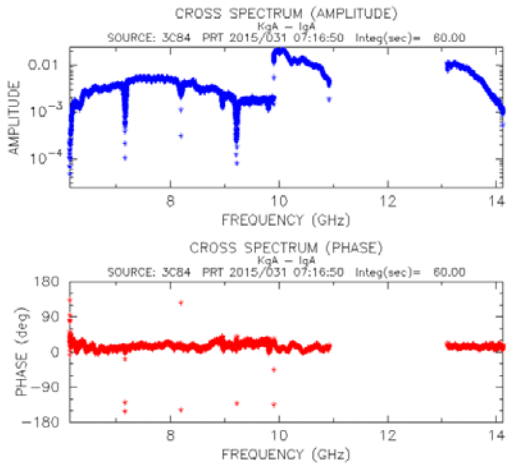

Figure 3. A cross spectrum after WBWS processing for the reference scan (PRT (processing reference time): 2015/031 07:16:50 UTC, source: 3C84, integration period: 60 sec).

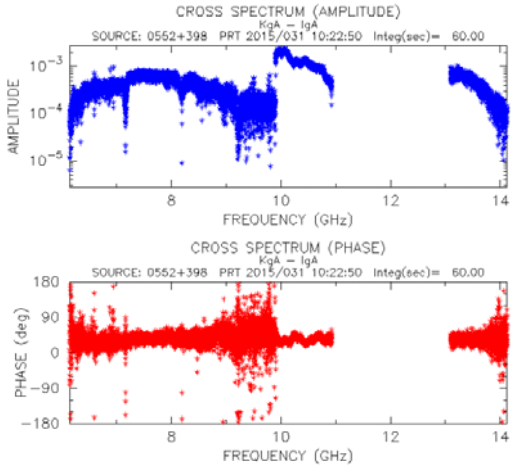

Figure 4. An example of WBWS processing for other scans (PRT (processing reference time): 2015/031 10:22:50 UTC, source: 0552+398, integration period: 60 sec).

$R(\tau, k)$ as follows.

1) get a cross spectrum $S(f, k)$ by Fourier transforming $R(\tau, k)$ where f is a frequency index.

2) get a cross spectrum $S_i(f, k)$ affected by ionospheric phase delay by calculating

$$S_i(f, k) = S(f, k) \exp[i\{\phi_{ion}(f) + \sigma_\phi\}]$$

where $\phi_{ion}(f)$ is given by

$$\phi_{ion}(f) = -2\pi\alpha\Delta TEC f^{-1}$$

and σ_ϕ is an additional phase noise to simulate a low signal to noise ratio case.

3) get $R_i(\tau, k)$ by inverse Fourier transforming $S_i(f, k)$.

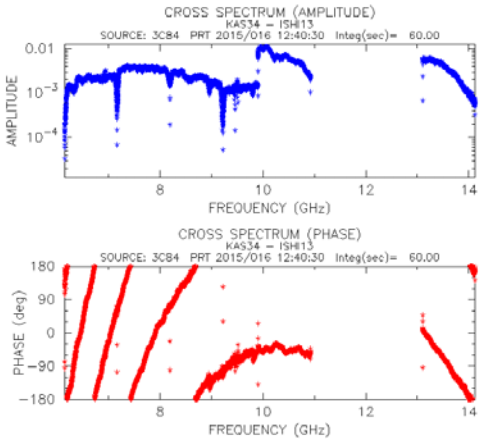

Figure 5. An example of cross spectrum after WBWS processing for simulated correlation data. Raw correlation data are observed on Jan.16, 2015 and set $\Delta TEC = 100$ TECU *for the simulation of ionospheric effect. Note that phase characteristics affected by the ionosphere can be seen.*

Fig.5 shows an example of cross spectrum after WBWS processing for simulated correlation data. In this case raw correlation data observed on Jan.16, 2015 are used to generate correlation data affected by the ionosphere and ΔTEC is set to 100 TECU (where TECU$= 1 \times 10^{16}/\mathrm{m}^2$). No additional phase noise is added. Note that phase characteristics affected by the ionosphere can be seen in the phase spectrum.

Fig.6 shows phase spectrum of phase model $\phi(f)$ (upper panel) and residual phase ($O - C$ where O: simulated data, C: model phase) (lower panel) after model fitting. ΔTEC and $\Delta\tau_{ion}$ are estimated as 100.4 TECU and 1.28 nsec, respectively. As shown in the result, ΔTEC used for generating simulated data is well reproduced. As for $\Delta\tau_{ion}$, it is fed back to an observed delay residual.

5. Conclusion

We have been developing the WBWS software and it has been almost completed. WBWS on the short baseline shows good results. As for the ionospheric correction, the test using simulated data demonstrates good results too. Actual evaluation should be carried out by using true long base line data such as an inter-continental baseline.

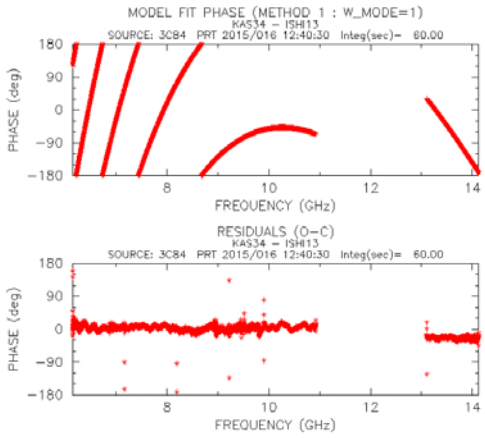

Figure 6. Phase spectrum of phase model $\phi(f)$ *(upper panel) and residual phase* $(O - C)$ *after model fiting (lower panel). Estimated* ΔTEC *and* $\Delta\tau_{ion}$ *are 100.4* TECU *and 1.28* nsec*, respectively.*

Acknowledgement: A wide band VLBI experiment was carried out with the cooperation of Geospatial Information Authority of Japan (GSI). We would like to thank GSI VLBI group for approving the use of Ishioka 13m antenna for this technical development.

References

Kondo, T. and H. Kunimori, III-5 bandwidth synthesizing software (KOMB), Rev. Radio Res. Lab., Vol.30, No.1, pp.199–216, 1984 (in Japanese).

Kondo, T., M. Sekido, and H. Kiuchi, 3.2.3 KSP bandwidth synthesizing software, J. Commun. Res. Lab., Vol.46, No.1, pp.67–76, 1999.

Broadband VLBI Data Acquisition System for GALA-V

Mamoru Sekido (*sekido@nict.go.jp*)
Kazuhiro Takefuji, Masanori Tsutsumi, and Tetsuro Kondo

NICT Space-Time Standards Laboratory,
Kashima Space Technology Center,
893-1 Hirai, Kashima Ibaraki 314-8501, Japan

Abstract: This paper describes two sorts of VGOS compatible broadband data acquisition systems (DASs) used in the GALA-V project. One is combination use of analog frequency converter and ADS3000+ sampler. This system enables narrow frequency channel observation compatible with conventional geodetic mode and 'NASA Proof of Concept' system developed by MIT Haystack. Another one is 'Direct Sampling' mode with high speed sampler K6/GALAS. Four broad channels of 1024 MHz width data are obtained at once by high speed sampling and its digital signal processing. Advantages of this method is not only simplicity but also stable phase relation among the broad channels. This is quite important for wide-band bandwidth synthesis for group delay derivation.

1. Introduction

NICT is conducting development of VGOS compatible broadband VLBI observation system for atomic frequency comparison project named GALA-V[1]. This project uses a pair of transportable small diameter antennas as the nodes for frequency comparison. Signal to noise ratio (SNR) of the VLBI observation with these nodes are enhanced by conjunction with joint observation of large diameter antenna and broad frequency range. This broad observation frequency range are designed to be compatible with VGOS system[2] for joint observation with VGOS stations. Two kinds of data acquisition systems (DASs) are used in the GALA-V project(Fig. 1). One is combination use of analog frequency conversion and digital baseband conversion (DBBC) sampler ADS3000+. Another one is using 'Direct Sampling' method[3] by using high speed sampler K6/GALAS.

Figure 2. Outlook picture (top) and backside view (bottom) of the ADS3000+ are displayed. External reference input of 10MHz(2),1PPS(1), and internal 10MHz(8) and 1PPS(13) are interfaced with BNC. RF signal inputs (3,4,5,6) are connected by SMA. Each of VSI-H output interface (9,10,11,12) supports data rate up to 2048 Mbps (64 MHz clock via 32 wires).

2. VOGS PoC compatible observation and DBBC sampler ADS3000+

Upper panel of Fig. 1 shows the case of combination use of analog frequency conversion and ADS3000+ in the GALA-V project. ADS3000+ is upgraded version of multifunctional sampler ADS3000[4]. Figure 2 shows the outlook of ADS3000+. After analog frequency down conversion of RF signal to intermediate frequency (IF),

Table 1. ADS3000+ Sampler Parameters.

Input	
Number of inputs	2
Input Freq. Range	0.01-1.5 GHz
Output	
Single Broad Channel Mode	128Msps :8 bit 512Msps : 2, 4 bit 1024Msps: 2 bit 2048Msps: 1 bit
Multi Channel DBBC Mode	No. of channels: 16 Rate: 4,8,16,32,64 Msps Bit: 1, 2, 4 bit
Max data rate/port	4096 Mbps
# output ports	4
Interface port	VSI-H
Control	telnet /1000BaseT

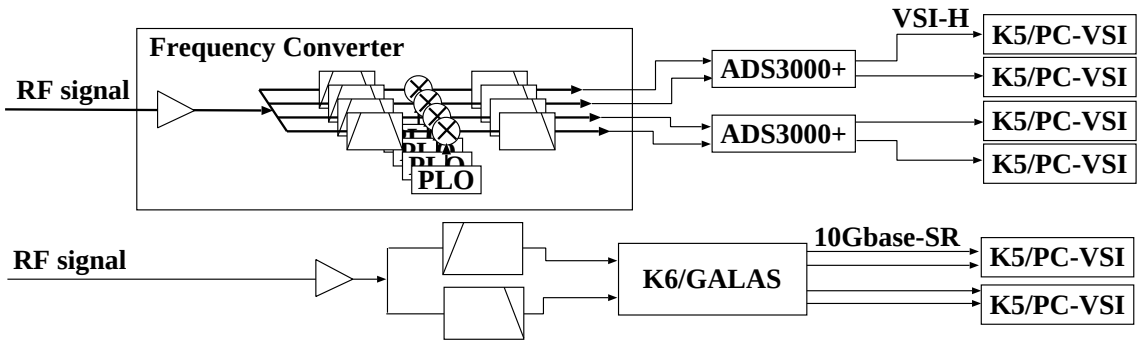

Figure 1. Two sorts of data acquisition systems in the GALA-V project. Upper figure shows combination of analog frequency conversion and IF sampling by using ADS3000+. Lower one is the case of 'Direct Sampling' by using high speed sampler K6/GALAS.

the IF signal below 1.5 GHz is fed into RF input of ADS3000+. By using digital baseband conversion (DBBC) function of ADS3000+, conventional multiple narrow channel data acquisition is carried out. That is compatible mode with 'NASA Proof of Concept' (PoC) VGOS system being developed by MIT/Haystack Observatory[5]. The ADS3000+ DBBC function extracts sixteen channels of specified frequency array. The bandwidth is chosen in any of 4, 8, 16, or 32 MHz. Frequency array can be specified by 1 Hz resolution. Upper side band (USB), lower side band (LSB), and complex data are selectable for output. For the PoC system compatible observation, 2048 Mbps (=64 Msps × 16 ch × 2bit) data acquisition is performed by single set of ADS3000+.

Basic observation mode GALA-V project is 1024 MHz width 'Broad Channel' data acquisition. Two data input ports of a ADS3000+ are used for capturing two IF signals in this case. Each of 2048 MHz sampling × 1 bit quantization data stream are output from each of two VSI-H interfaces. Thus the output can be recorded by any of the VSI-H[6] compliant data input module(DOM). We uses the K5/VSI systems for recording the VSI-H data stream of ADS3000+. The K5/VSI system is composed of PC-VSI card and high data rate recoding system with RAID disk drives[7]. Parameters to represent performances of the ADS3000+ sampler is summarized in Table 1.

2.1 Direct Sampler K6/GALAS

Lower part of the figure 1 shows another way of data acquisition named 'Direct Sampling'[3]. Analog radio frequency (RF) signal up to 16 GHz is fed into two inputs of the sampler. Each of the signals are converted to digital data by using sampler

Table 2. K6/GALAS Sampler Parameters.

Input	
Number of inputs	2
Input Freq. Range	0.1 – 16.4 GHz
Output	
Single Broad Channel Mode	3200 Msps :1, 2 bit 6400 Msps : 1, 2 bit 12800 Msps: 1 bit
Multi Channel (DBBC) Mode	Nch: 1, 2, 3, 4 Rate: 2048 Msps Bit: 1, 2 bit
Max data rate/port	8,192 Mbps
# Output port	4
Output Interface	10GBASE-SR (SFP+)
Data format	VDIF/VTP over UDP/IP
Control	telnet/1000BaseT

K6/GALAS of 16,384 MHz sampling 3bit quantization. Then signal of 1024 MHz width at specified frequency band is extracted by DBBC function of the sampler. Frequency bands to be extracted is specified by 1kHz resolution, and one set of K6/GALAS outputs four data streams of 2048 Mbps (2048 Msps ×1 bit). Output data packets formatted in the VDIF format[8] are transmitted from 10GBASE-SR optical fiber network by the VTP/UDP/IP protocol. Figure 3 indicates outlook of the direct sampler K6/GALAS. Output data stream of the K6/GALAS is captured by a off-the-shelf computer set equipped with 10GBASE-SR interface and RAID-5 disk array system. Software package for receiving and transmitting VDIF/VTP data stream has been developed by our group as 'VDIF/VTP Software Suite'[9], and it is freely

Figure 3. Upper figure shows outlook of direct sampler K6/GALAS. Radio frequency analog signal is converted to digital signal by 16,384 MHz sampling 3 bit quantization. Specified four 1-GHz bandwidth signals (2048Msps × 1bit × 4 bands) are extracted via digital baseband conversion function. The data is output in the stream of VIDF/UDP packets from 10GBASE-SR interfaces. Lower figure shows backside view of the sampler. Sampling clock is selection by connecting one of clock outputs at (1) and (3) to clock input (2). 3.5mm connectors (4)-(5) are RF singal inputs. External reference 10MHz signal and 1PPS are input from (9) and (6), respectively. Returning 1PPS (7) and internal 1PPS (8) are also available. Four 10GBASE-SR interfaces (10)-(11) are for data output and 100Base-T Ether connector (12) is used for external control.

available from a web page[1] Table 2 shows the sampling parameter of K6/GALAS.

3. Discussion

3.1 Broad Channel and Multiple Narrow Channel Data Acquisition

There are advantages and drawbacks in each of 'Broad Channel' and 'Multiple Narrow Channel' data acquisition. The important advantage of 'Multiple Narrow Channel' data acquisition is the backward compatibility with the conventional geodetic VLBI mode. Mixed observation of conventional S/X and VGOS will be necessary in transition from conventional geodetic observation system to the VGOS. It is important especially from view point of stability of the global VLBI solution of terrestrial reference frame. Disadvantage of 'Multiple Narrow Channel' mode is complexity of signal synthesis of the many channels. It requires accurate and stable Phase-calibration (P-CAL) system for coherent synthesis of the signals in separate channels.

In case of 'Broad Channel' mode, continuous 1024 MHz bandwidth signal is acquired in a single channel. P-CAL signal is not always necessary for intra-band phase correction. Bandpass phase characteristic can be obtained by cross correlation spectrum of strong radio source as a reference. If we could assume the bandpass phase characteristic is stable, phase characteristics of observation system is calibrated by using the reference cross spectrum.

Regarding on inter-band phase correction for coherent broad bandwidth synthesis, P-CAL should be necessary especially in case using multiple IF samplers after analog frequency conversions. But it is not always the case of 'Direct Sampling' method. Because if signal in the whole frequency range is digitized by single sampling, then inter-band phase relation should be more stable than analog frequency conversion using phase-lock oscillators and mixers. If 'Direct Sampling' system is stable, we can avoid using P-CAL signal for inter-band bandwidth synthesis. Even in that case, P-CAL signal is useful for monitoring the system stability. Advantage of 'Direct Sampling' in the broadband bandwidth synthesis is described in latter section and article by T.Kondo[10].

GALA-V project uses the 'Broad Channel' observation as basic observation mode. Also 'Multiple Narrow Channel' compatible observation mode is supported as a option for joint observation with VGOS station of 'PoC' DAS. Table 3 summarizes the observation modes of samplers of GALA-V project and VGOS 'PoC' compatible mode.

3.2 Direct Sampling and Conventional Analog Frequency Conversion

There are several advantages in 'Direct Sampling' method especially for broadband delay observation. The simplicity of the system is obvious from Fig.1. Number of the components and analog system for data acquisition is reduced. Not only the simplicity, essential advantage of 'Direct sam-

[1] http://www2.nict.go.jp/aeri/sts/stmg/K5/Software/VDIF_SUDP/VDIF-SUDP-j.html

Table 3. Observation modes of the Samplers in GALA-V project and VGOS compatible mode.

Samplers	ADS3000+	K6/GALAS
Narrow Channel mode ('NASA PoC' compatible)	64Msps x 16 ch x 2bit Total: 2048 Mbps	N.A.
Broad Channel Mode	2048Msps x 2band x 1bit Total: 4096 Mbps	2048 Msps x 4 band x 1 bit Total: 8096 Mbps
Data Output	PC-VSI or any recorder with VSI-H interface	10GBASE-SR interface, VDIF/UDP or VDIF/VTP

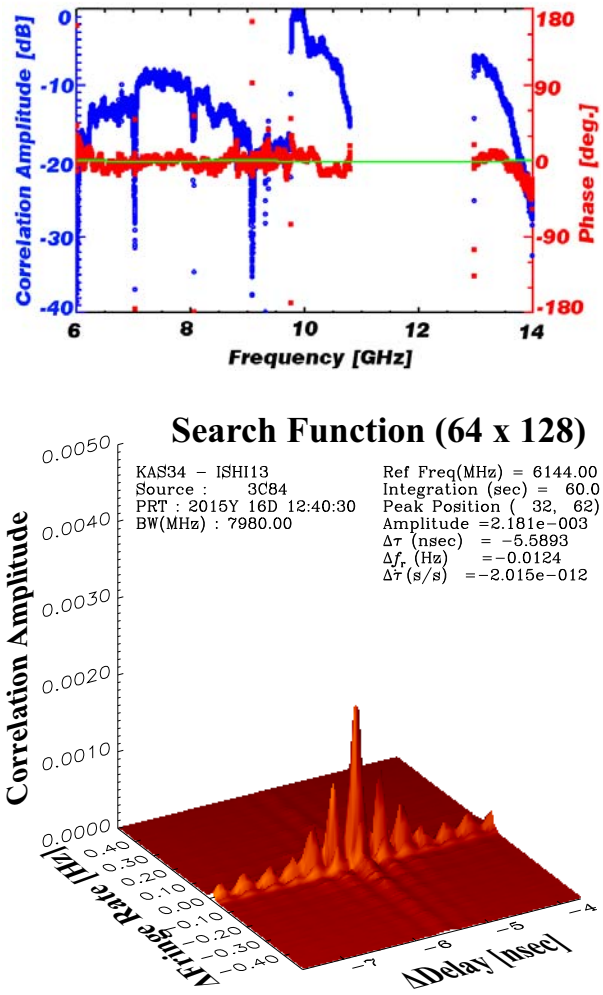

Figure 4. Cross Spectrum(Amplitude & Phase) of broadband VLBI observation between Kashima 34m – Ishioka 13m on 30 Jan. 2015(upper panel), and Fringe of the broad bandwidth synthesis over 8 GHz bandwidth(lower pannel).

pling' method is that the RF signal properties of phase and amplitude in whole frequency range are frozen at the time of A/D conversion. Then digital filtering and other signal processing are applied. It is ideal way in future VLBI data acquisition, even though there is space for improvement in the limited level of quantization in current system.

This advantage might play a key role in derivation of broadband delay observable. Broad bandwidth synthesis to derive group delay requires coherent property of the correlation signal over broad frequency range. Phase may potentially change over broad frequency range due to characteristic of microwave components and over time due to various reasons such as temperature, humidity, mechanical stress on the cables, and so on.

In case of conventional analog frequency conversion, each signal of 1 GHz frequency width passes through independent analog components. Thus P-CAL stability is quite important for coherent synthesis of broadband signal.

In case of 'Direct sampling', since phase information is frozen at the sampling point over whole frequency band, coherence degradation can be avoided after sampling point in principle.

To demonstrate the advantage of 'Direct Sampling', We have made a broadband VLBI experiment on Kashima 34m - Ishioka 13m[11] baseline in Jan. 2015. Six 1 GHz bandwidth signals were acquired over 6 GHz – 14 GHz frequency range. Two broad channels were acquired with single broad channel mode of ADS3000+, and other four broad channels were captured with multi channel DBBC mode of direct sampler K6/GALAS. Correlation processing was made on the data of each band by using software correlator GICO3[12], which was originally developed by M.Kimura and updated by K.Takefuji of NICT. Then correlation outputs were synthesized over the broad frequency range by upgraded bandwidth software "KOMB"[13, 10]. Figure 4 shows the cross spectrum and the fringe obtained by this wide-band bandwidth synthesis (WBWS) over 8GHz width. Theoretical group delay precision expected from this 8 GHz width

bandwidth synthesis reached to 27 femto seconds in this experiment. This WBWS was successfully achieved without using P-CAL signal but relying on the phase stability of the acquisition system. Please refer to papers[10, 13] for detailed procedure of the WBWS.

4. Summary

Broadband data acquisition systems developed for the GALA-V project were described in this paper. The advanced characteristic of 'Direct Sampling' method was discussed and demonstrated in short baseline broadband VLBI observation between Kashima 34m and Ishioka 13m radio telescopes. Direct sampling has potentially great advantage for broadband VLBI observation. The validity of this method have to be examined by real VLBI observations.

References

[1] Sekido, M., et al., "Development of Wideband VLBI system (Gala-V)", proceedings of IVS 2014 General Meeting "VGOS: The New VLBI Network" Edited by Dirk Behrend, Karen D. Baver, and Kyla L. Armstrong Science Press (Beijing) ISBN 978-7-03-042974-2, pp.77-81, 2014

[2] Petrachenko, B., et al., "Design Aspect of the VLBI2010 System: Progress Report of the VLBI2010 Committee", NASA/TM-2009-214180, 2009.

[3] Takefuji, K., et al., "High-order Sampling Techniques of Aliased Signals for Very Long Baseline Interferometry", PASP, Vol.124, pp.1105-1112, 2012.

[4] Takeuchi, H., et al., "Development of a 4 Gbps Multifunctional Very Long Baseline Interferometry Data Acquisition System", PASP, Vol. 118, pp.1739-1748, 2006.

[5] Niell,A., et al., "VGOS Operations and Geodetic Results", Proceedings of IVS 2014 General Meeting "VGOS: The New VLBI Network" Edited by Dirk Behrend, Karen D. Baver, and Kyla L. Armstrong Science Press (Beijing) ISBN 978-7-03-042974-2, pp.97-101, 2014

[6] Whitney, A., "VLBI Standard Hardware Interface Specification -VSI-H", `http://vlbi.org/vsi/`, 2000.

[7] Kimura, M., J. Nakajima, "The implementation of the PC based Giga bit VLBI system", IVS NICT-TDC News. Vol. 21, pp.31-33, 2002.

[8] Whitney, A., M. Kettenis, C. Phillips, and M. Sekido, "VLBI Data Interchange Format (VDIF)", Proceedings of IVS 2010 Gleral Meeting "VLBI2010: From Vision to Reality" Edited by Dirk Behrend and Karen D. Baver NASA/CP-2010-215864, pp.192-196., 2010.

[9] Sekido, M., et al., "Development of an e-VLBI Data Transport Software Suite with VDIF", Proceedings of IVS 2010 General Meeting "VLBI2010: From Vision to Reality" Edited by Dirk Behrend and Karen D. Baver NASA/CP-2010-215864, pp.410-414., 2010

[10] Kondo, T., and K. Takefuji, "On a Wide-Band Bndwidth Synthesis II" IVS NICT-TDC News No.35, pp.23-27, 2015.

[11] Fukuzaki, Y., et al., "Receiving Performance of Ishioka VGOS Antenna", IVS NICT-TDC News, No.34, pp.8-10, 2014.

[12] M.Kimura, "Development" of the software correlator for the VERA system II", IVS NICT-TDC News. No.28, pp.22-25, 2007.

[13] Kondo, T., and K. Takefuji, "On a Wide-Band Bndwidth Synthesis" IVS NICT-TDC News No.34, pp.23-27, 2014.

Development of Wideband Feed

Hideki Ujihara (*ujihara@nict.go.jp*), Kazuhiro Takefuji and Mamoru Sekido

Kashima Space Technology Center, National Institute of Information and Communications Technology, 893-1 Hirai, Kashima, Ibaraki 314-8501, Japan

1. Status of development

New wideband feed has been installed in 34m antenna in this summer. The name of this new feed is NINJA feed, because of flexibility in its beam width. It was designed for 3.2-14.4GHz and was mounted nearby the prototype of IGUANA Daughter feed which is for higher frequency, 6.5-15GHz. (Fig.1).

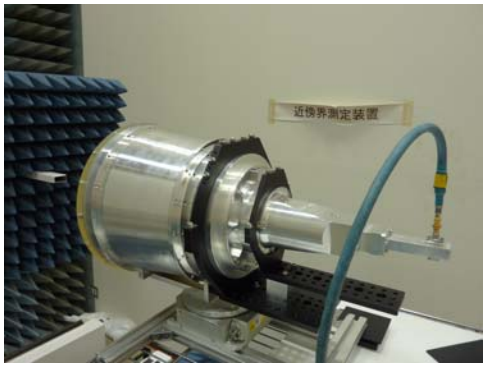

Figure 1.NINJA Feed for kashima 34m antenna

The NINJA feed is a type of lensed horn (Fig.1), which was arranged from a wideband feed for center parabola focus of MARBLE. Two lenses make the beam width narrower to fit cassegrain focus of 34m antenna Now this feed has been mounted with WRD350D36 waveguide-SMA converter for only single linear polarization. Its return loss is shown in (Fig.3).

However, newly developed SMA converter for dual polarization will replace it. Simulation models of the converter have still some resonances (Fig.4),(Fig.5), however they will be removed in few month.

Also, the optics of MARBLE, small VLBI stations with 1.5m and 1.6m dishes, will be replaced by 2.4m cassegrain optics with NINJA feed. Distortion of the dish and whole structure was estimated with COMSOL, not to grow its weight too much. The mass of new optics will be twice of current systems.

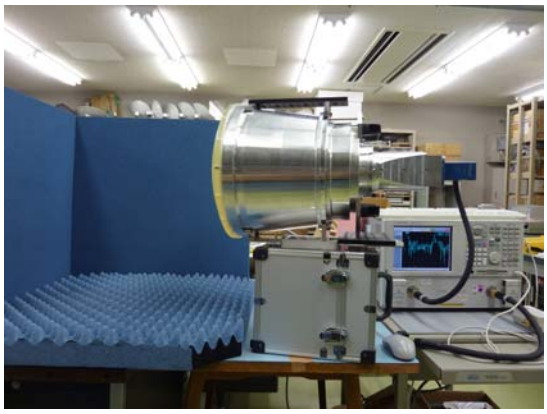

Figure 2.
New feed with WRD350D24-SMA output.

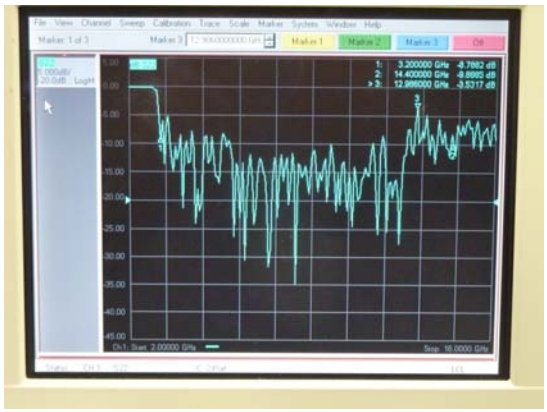

Figure 3.
Return loss of New feed with WRD350D36-SMA output.

2. Plans

Complete IGUANA feed is still delayed due to production schedule of its complexed waveguides and structure. However, in 34m antenna, we can use 6.5-15GHz with the prototype daughter feed and NINJA feed for 3.2-14.4GHz.

Dual polarization output will be installed in 2015 for replacement of single-pol output and a DWDM RF over Fiber-link system for dual-pol will be set in 34m antenna.

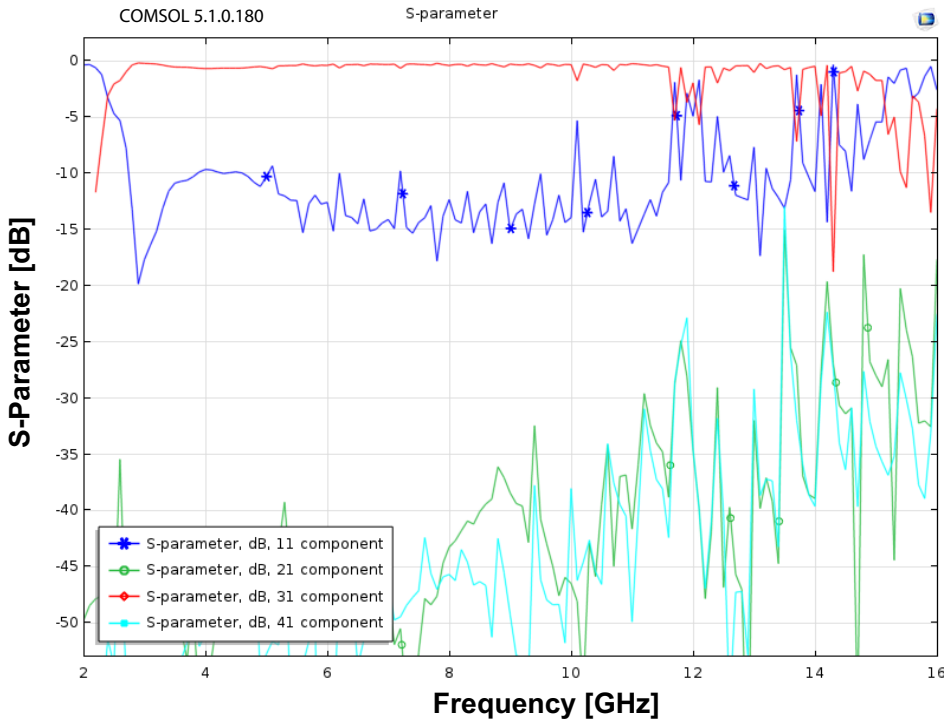

Figure 4. S-paramters with port 0 input

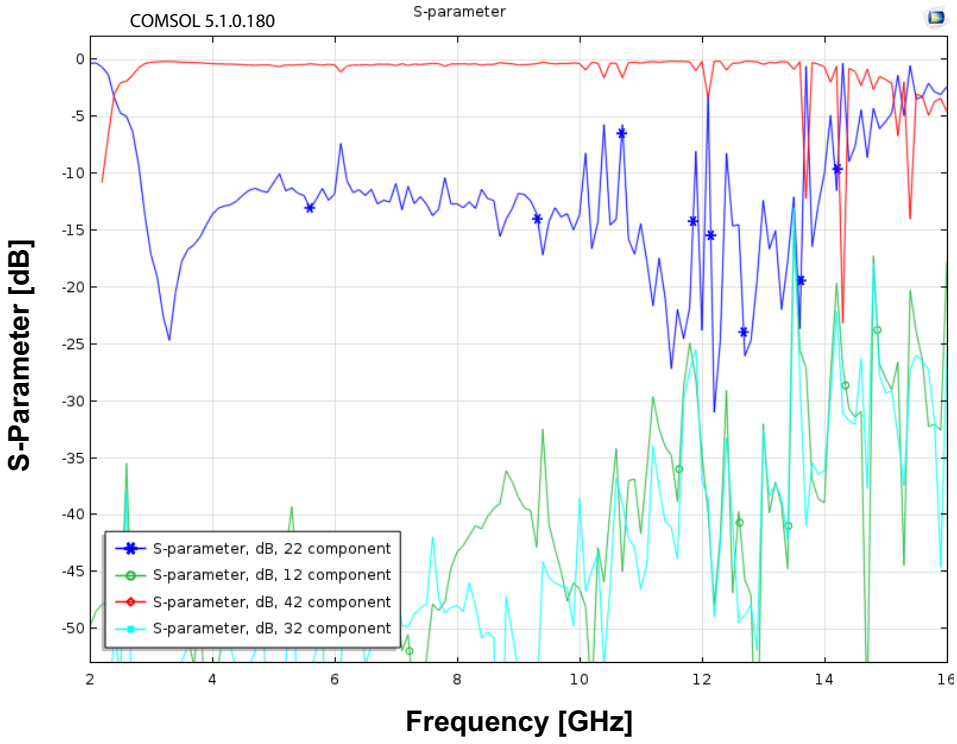

Figure 5. S-parameters with port 1 input

Report on the Test Observation of Hitachi-Takahagi Interferometer

Rinichi Kako, Munetake Momose, Yoshinori Yonekura, Koichiro Sugiyama
Ibaraki Univ., 2-1-1 Bunkyo, Mito, Ibaraki, Japan

Tetsuro Kondo, Mamoru Sekido
NICT, 893-1 Hirai, Kashima, Ibaraki, Japan

Abstract: Hitachi-Takahagi interferometer is being started up since 2013. This system will enable to make long-term monitoring observation of continuous wave objects. Last year, correlator which connects each station by optical fiber cables and correlates in real time, has been introduced. Then, we started evaluation of this correlator and K5/VSSP system.

1. Introduction

Hitachi and Takahagi antenna have been used for Japanese VLBI Network or single dish observation. Table 1 is the location of these antennas.[1] Now, two interferometric systems have been introduced. One is the K5/VSSP system, composed of K5/VSSP32 sampler and correlation software. The other is the hardware correlator, correlate in real time.

2. Test Observations and Results for the K5/VSSP System

In Aug. 14, 2013, we made observations of 3C273B by interferometer of K5/VSSP system. Specification of observations is shown in Table 2.

Figure 1 shows correlative phase and amplitude, indicating that these changed sinusoidally. Typical period of this sinusoidal change is 1-2 second, and it varies every hour, in other words, it depends on source position. It is conceivable that sinusoidal fluctuation is caused by fringe residual error. Base line length of this interferometer is very short, about 260 m, and fringe rate is about 0.5 Hz. So we made observations with the configuration that the LO of Takahagi is 10 kHz lower than that of Hitachi. Figure 2 shows the result of this experiment indicating that sinusoidal fluctuation has been averaged.

Figure 3 shows the result of the observation of methanol maser 188.9+08. It shows that amplitude line was divided into two components, broad and narrow ones, and phase line was split into two components, which are separated 180 degree each other. This problem was caused by the relation between FFT points and the lag window. Now K5/VSSP system's correlation software has been updated, adding option for line spectrum, and this problem has been solved.

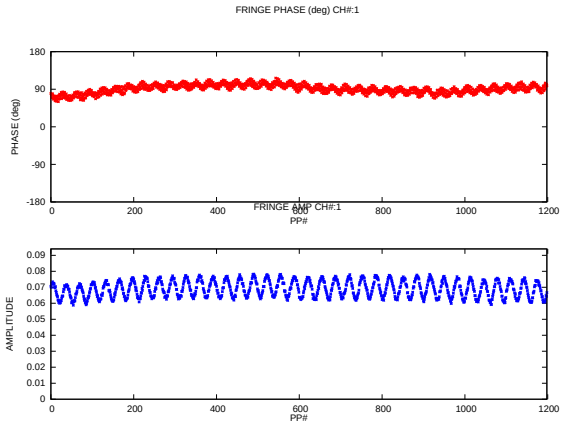

Figure 1. The result of observation of 3C273B. Upper diagram shows fringe phase, and lower shows amplitude. Phase and amplitude vary sinusoidally.

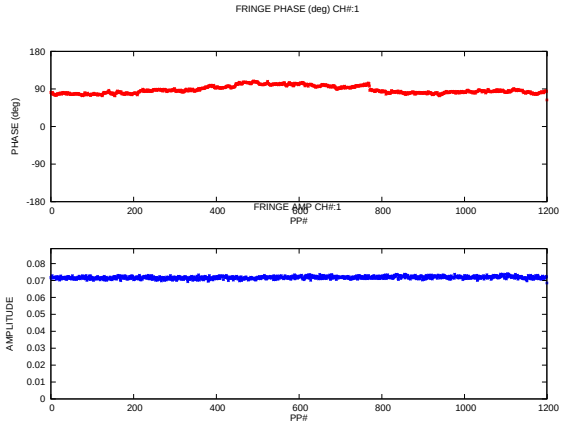

Figure 2. Fringe phase and amplitude by the observation with the configuration that LO of Takahagi is 10 kHz lower than that of Hitachi.

3. Test Observations and Results for Hardware Correlator

Hardware correlator has been introduced in 2014, and the first light was achieved in Mar. 3, 2015 (Figure 4). Then, we find that intense noise at IF frequency of ∼560 MHz contaminates and breaks correlation, and fringe phase change every moment. We found that the cause of the noise is an influence of artificial radio wave for ∼6530-6570 MHz. The Hitachi and Takahagi antenna use 1st LO of 6088 MHz and convert 6600-7112 MHz to 512-1024 MHz. However, the passband of the band

Table 1. Antenna location[1]

	X [km]	Y [km]	Z [km]
Hitachi	-3961.788796	+3243.597525	+3790.597709
Takahagi	-3961.881647	+3243.372513	+3790.687466
Base line length: 259.438 m			

Table 2. Specification of K5/VSSP system observations

Source	3C273B	3C273B	188.9+08
Date	2013/8/14 (226)	2015/1/8 (008)	2015/1/13 (013)
Band	8448 - 8480 MHz	8448 - 8480 MHz	6664 - 6696 MHz
	···	Takahagi LO is 10 kHz lower than Hitachi	···
Sampling rate	64 MHz	64 MHz	64 MHz

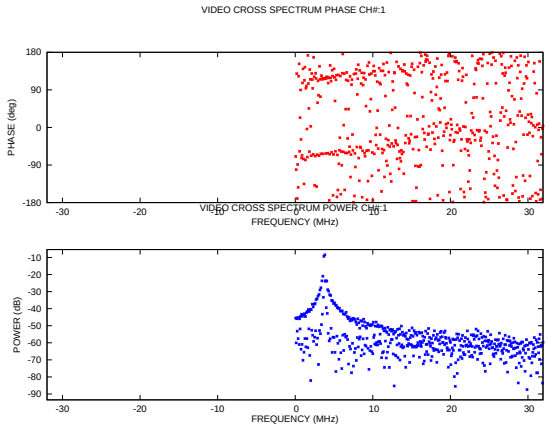

Figure 3. The result of observation methanol maser 188.9+08. Phase splits in two, and amplitude overlaps.

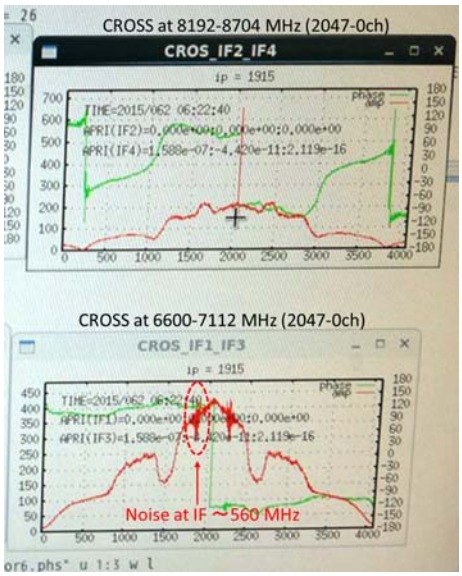

Figure 4. Hardware correlator first light. Red line shows amplitude, and green line shows fringe phase. It shows that noise arises at IF frequency of ∼560 MHz.

pass filter was 300-1100 MHz, resulting that the leakage of the noise at ∼6530-6570 MHz into the IF frequency of ∼442-482 MHz. This contaminates the correlated results at ∼542-582 MHz, since the sampling rate was 1 GHz and no digital filter was used. Now, new band pass filter with the passband of 550-950 MHz has been introduced, and problem of the noise contamination was cleared.

Fringe rotation was caused by the firmware defect. Updated firmware has been installed, and this problem is resolved.

4. Summary

Test observations for K5/VSSP system and hardware correlator have been done from 2013. For K5/VSSP system, problems that amplitude and phase vary sinusoidally and split for line spectrum occurred. Varying would not be the effect of K5/VSSP system because its period is 1-2 second and was solved by using different LO frequency for two antennas. Splitting has been solved by adding option to the correlation software. For hardware correlator, intense noise and fringe phase rotation occurred. Noise was filtered out by the new band pass filter. Fringe rotation was caused by a firmware bug. Now, this bug was fixed.

Acknowledgment

We are grateful to NICT for the use of correlation software.

References

[1] Yonekura, Y., Present Status of Ibaraki station (Takahagi and Hitachi 32m Radio Telescopes), IVS NICT-TDC News No.33, 6-7, 2013.

Observation of Jupiter's Synchrotron Radiation in the Magnetospheric Variation Period : Preliminary Results

Hiroaki Misawa[1]
(*misawa@pparc.gp.tohoku.ac.jp***),**
F. Tsuchiya[1], **S. Satoh**[1], **H. Kita**[1],
M. Sekido[2], **K. Takefuji**[2], **E. Kawaii**[2],
T. Kondo[2] **and S. Hasegawa**[2]

[1]*Planetary Plasma and Atmospheric Research Center, Tohoku University, 6-3 Aoba, Aramaki, Aoba-ku, Sendai Miyagi, Japan*
[2]*NICT Space-Time Standards Laboratory, Kashima Space Technology Center, 893-1 Hirai, Kashima Ibaraki, Japan*

Abstract: Rapid variation of relativistic electrons in Jupiter's radiation has been inferred with the time scale of a day or less from the observation of Jupiter's synchrotron radiation (JSR) at 327MHz. The Galileo Jupiter orbiter data showed this rapid variation has some relation with the magnetic reconfiguration events (MRE) in the outer magnetosphere, however, the causality of the rapid variation of JSR and MRE have not been known yet. One plausible causality for MRE is proposed to be enhancement of mass loading originally brought by enhancement of plasma originated from Io. In the middle of Jan. to May, 2015, obvious Io plasma enhancement has been identified by earth-based optical observations. This phenomena gives us a good opportunity to directly confirm the relation between the occurrence of rapid variation of Jupiter's radiation belt and enhancement of the Iogenic plasma. We have made a quasi regular JSR observation at 2.3GHz for about three weeks in March, 2015. We report a preliminary result of this JSR observation.

1. Introduction

It is known that Jupiter has a radiation belt filled with relativistic particles like the Earth, though the flux and energy of the particles are much larger. The relativistic particles are trapped by Jupiter's intense magnetic field and emanate synchrotron radiation. Thus the radio emission (hereafter we call it JSR) has information on dynamics of Jupiter's deep inner magnetosphere. The Tohoku University group has started regular JSR observations since 1990's and revealed that JSR has short term variations with the time scale of several days [1] and such the short term variations are general in several hundreds MHz [2,3]. The characteristic time scale of several days has not been explained by previous understandings for Jupiter's radiation belt particles; i.e., the characteristic time scale of representative source process is about two years for the case of radial diffusion of energetic electrons [4] and that of loss process is more than 10 days as the shortest case for the interaction with Jupiter's moons [5]. To interpret this problem, Miyoshi et al. (1999) [1], Bhardwaj et al. (2009) [6] and Tsuchiya et al. (2011) [3] showed that the time scale meets with the enhanced radial diffusion for the relativistic particles caused by the solar UV/EUV heating to Jupiter's upper atmosphere as originally proposed by Brice and McDonough (1973) [7]. And Kita et al. (2015) showed that a short term JSR variation occurred in sync with temperature enhancement of Jupiter's upper atmosphere during the solar UV/EUV increasing phase [8].

On the other hand, JSR sometimes shows more rapid flux variations (RFV) by more than several tens % whose characteristic time scale is a day or less. It is quite difficult to explain its physical processes by present theories even though the enhanced radial diffusion mentioned above. From the JSR observation at 327MHz for the period of the Galileo Jupiter orbiter exploration, Misawa et al. (2013) suggested that some RFV events occurred in sync with the magnetic reconfiguration event (MRE) [9] which is a global magnetospheric reccurent disturbance with the repetition period of 2∼6 days [10,11,12]. Although a driving force of MRE has been not understood well, enhancement of plasma mass loading originally brought by enhancement of Iogenic valcanic gases is proposed as a plausible candidate [13]. So far there has been no observational evidence showing reliable relationship between occurrence of RFV and enhancement of plasma mass loading phenomena.

In the middle of Jan. to April, 2015, remarkable Iogenic gas and plasma enhancements have been identified by a ground-based optical observation [14] and the Hisaki space telescope satellite [EXCEED/Hisaki Science team, private communication]. This phenomena gives us a good opportunity to directly confirm the relation between the occurrence of RFV and Iogenic plasma. We have

made a quasi regular JSR observation at 2.3GHz for about three weeks in March, 2015. In this paper, we report a preliminary result of the JSR observation with brief explanation of the newly developed spectrum analysis for reducing influence of RFI (Radio Frequency Interference).

2. Observation

The observation of JSR had been made using the Kashima 34-m radio telescope at S-band from Mar. 4 to 24, 2015 everyday except 8 to 12 and 21. Our research group has made JSR observations several times using this system since 1997 [1]. In these previous observations, we have utilized a power meter to derive the total flux for the wide IF band. However, we utilized a spectrum analyzer in this time to avoid RFI affecting estimation of the total flux of JSR whose usual flux density is several Jy. We sampled the IF band (∼190 MHz) with the resolution bandwidth of 1MHz every 2 sec. An example of the sampled spectrum for an hour is shown in Figure 1.

In the observation of JSR, we made the drift scan for Jupiter repeatedly every 6.5 minutes and made calibration of system gain and receiver noise temperature before and after each drift scan by the Y-factor method. We also inserted observations for radio flux density calibrators such as 3C123, 3C161 and 3C218, and sky-tipping for the azimuthal direction of the radio flux density calibrators and Jupiter roughly every 1 hour. The JSR observation had been made for about 9 hours everyday for the elevation of Jupiter more than roughly 30 degrees.

3. Data Analysis

In the data analysis, firstly RFIs are eliminated from the raw spectrum; i.e., wide band RFIs are eliminated by visual inspection and narrow band RFIs are eliminated by a median filtering method with the bandwidth of 5 MHz. An example of the total flux observation for a radio source (3C123) using this method is shown in Figure 2, where the blue line is the averaged power for the full IF band and the red line is that for the RFI eliminated IF band. In the figure, some power offset is added to the red line so that the effect of the RFI elimination can be seen easily. Secondly, received power of Jupiter's radio emission was derived from each drift scan data using the Gaussian fitting method. Thirdly, the gain of the received power level was

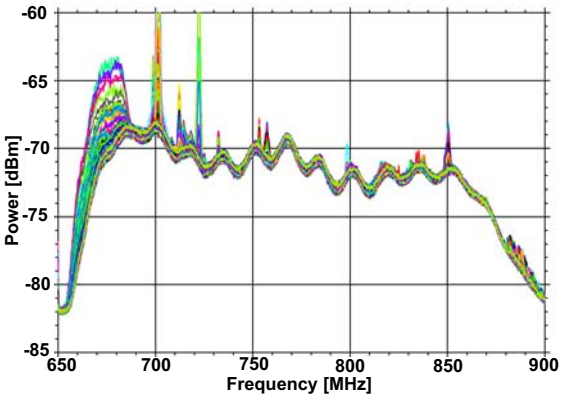

Figure 1. Example of the observed spectra sampled every 2sec and overlaid for an hour. The data were taken in the evening of Mar. 4, 2015 when the radio telescope was pointed to the east southeast at an elevation angle of 40–70 degrees.

calibrated using the result of the Y-factor method. Fourthly, the calibrated power level should be compensated using the atmospheric extinction factor derived by the sky-tipping (at present unexecuted). Fifthly, absolute radio flux was estimated by comparison with radio flux calibrators. Sixthly, the radio flux was standardized to that at a distance of 4.04 AU which is the generally used mean closest distance between the earth and Jupiter. Finally JSR flux was derived by reducing the radio flux of the thermal component of Jupiter at S-band; i.e., 2.02 Jy at 4.04AU [15].

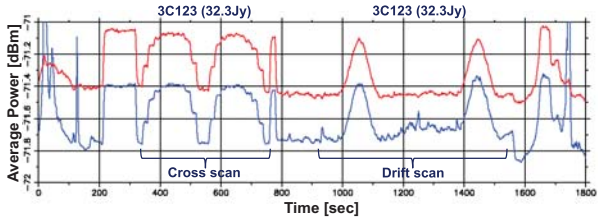

Figure 2. Example of the total flux observation for the radio galaxy 3C123 at S-band using a spectrum analyzer connected to the IF output of the Kashima 34-m radio telescope. The blue line is the averaged power for the full IF band and the red line is that for the RFI eliminated one.

4. Results and Discussions

The result of derived JSR flux is shown in the top panel of Figure 3. Each JSR flux was estimated as an averaged value between the radio flux

calibrations; i.e., roughly every one hour. The error bars were estimated as the standard deviations for the JSR flux values. It is well known that the total JSR flux shows apparent periodic variation in sync with Jupiter's rotation by about 10% [16], and the apparent variation should be compensated to determine actual total JSR flux [see 1,17]. However, at present the compensation has not been performed, and simple averaged flux values are plotted in the figure. In the bottom panel of Figure 3 the daily solar 10.7cm radio flux (F10.7) expected at Jupiter is shown, where solar F10.7 is known as a good proxy of solar UV/EUV flux. From Figure 3, it is shown that there were some short term variations by roughly more than 20% of the normal flux level and the variations has little correlation with those of F10.7: The F10.7 variations showed gradual decrease and increase especially after Mar. 9, while the JSR flux variations showed bumpy nature with the time scale of roughly a few days. This result implies that the variations were not apparent ones with Jupiter's rotation, but actual ones driven by some processes possibly faster than the solar UV/EUV heating effect.

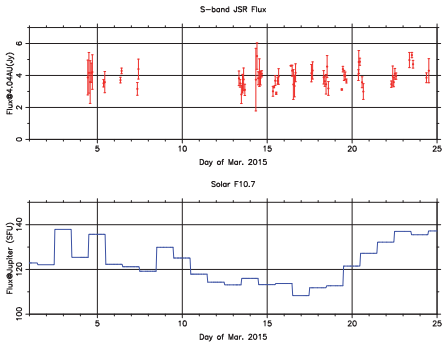

Figure 3. Result of the JSR flux observations at S-band (top panel) and solar 10.7cm radio flux expected at Jupiter (bottom panel) in Mar., 2015. There was no JSR flux observation for Mar. 8 - 12 and 21 due to the other experiments on the Kashima system.

As mentioned in Introduction, remarkable Iogenic gas and plasma enhancements have been identified in the middle of Jan. to April, 2015 [14 and Tsuchiya et al., private communication]. During this period, the Hisaki observation also revealed that Jupiter's auroral intensity showed some transient variations [EXCEED/Hisaki Science team, private communication]. It is known that Jupiter's transient aurora variations are brought by two different processes; i.e., one is externally triggered by compression by solar wind [e.g. 18] and another one is driven by some internal plasma circulation processes [19]. Kimura et al. (2015) suggested that the characteristic duration time of auroral intensity variations is different for these two auroras; that of the externally driven type is a few days, while that of the internally driven type is roughly less than a half day (∼ one Jupiter's rotation period) [19]. In the JSR observation period in March, 2015, the duration time of almost all transient auroras is less than a half day and the transient auroras occurred quasi periodically at an interval of 2-4 days, which is nearly the same time scale as the previously observed MRE [10,11,12]. These observation results strongly suggest that some internal plasma circulation processes dominantly occurred during the JSR observation period, though variations of solar wind compressions on Jupiter occurred several times in the same period (courtesy of C. Tao).

Due to unevaluation of atmospheric extinction and apparent variation by Jupiter's rotation, confirmation of occurrence of RFV during the remarkable gas and plasma enhancement period and also that of correspondence between the quasi periodic auroral variations and JSR flux variations are deferred for future analyses. However the observed distinctive auroral features (probably) related to the Iogenic gas and plasma enhancement much encourage our expectancy for revealing how deep the MRE affects the inner magnetosphere.

5. Acknowledgments

We express our sincere thanks for all staffs of NICT Space-Time Measurement Group, Kashima Space Technology Center for their assistance on the JSR observation. We also acknowledge NASA/GSFC's Space Physics Data Facility's OMNIWeb service for the use of solar 10.7cm radio flux data. This work was carried out by the joint research program of the Solar-Terrestrial Environment Laboratory (the Institute for Space-Earth Environmental Research after Oct. 2015), Nagoya University.

References

[1] Miyoshi, Y. et al., Observation of short - term variation of Jupiter's synchrotron radiation, Geophys. Res. Lett., Vol.26, pp.9–12, 1999.

[2] Misawa, H., and A. Morioka, Observations of Jovian decimetric radiation at a frequency of 327 MHz, Adv. Space Res., Vol.26, pp.1537–1540, 2000.

[3] Tsuchiya, F. et al., Short-term changes in Jupiter's synchrotron radiation at 325 MHz: Enhanced radial diffusion in Jupiter's radiation belt driven by solar UV/EUV heating, J. Geophys. Res., Vol.116, doi:10.1029/2010JA016303, 2011.

[4] de Pater, I., and C. K. Goertz, Radial diffusion models of energetic electrons and Jupiter's synchrotron radiation: 2. Time variability, J. Geophys. Res., Vol.99, pp.2271–2287, 1994.

[5] Santos-Costa, D., and S. A. Bourdarie, Modeling the inner Jovian electron radiation belt including non - equatorial particles, Planet. Space Sci., Vol.49, pp.303–312, 2001.

[6] Bhardwaj, A. et al., GMRT observation of Jupiter 's synchrotron radio emission at 610 MHz, in The Low - Frequency Radio Universe, edited by D. J. Aaikia et al., Astron. Soc. Pac. Conf. Ser., Vol.407, pp.369–372, 2009.

[7] Brice, N. M., and T. R. McDonough, Jupiter's radiation belts, Icarus, Vol.18, pp.206–219, 1973.

[8] Kita, H. et al., Relation between the short-term variation of the Jovian radiation belt and thermosphere derived from radio and infrared observations, J. Geophys. Res., in printing.

[9] Misawa, H., and T. Mizuguchi, Short-term variation phenomena in Jupiter's radiation belt: Their relation with the magnetospheric events, Proc. Symp. Planet. Science 2013, SPS2013-57, 2013.

[10] Woch, J. et al., Quasi-periodic modulations of the Jovian magnetotail, Geophys. Res. Lett., Vol.25, pp.1253–1256, 1998.

[11] Louarn, P. et al., A study of the large-scale dynamics of the Jovian magnetosphere using the Galileo plasma wave experiment, Geophys. Res. Lett., Vol.25, pp.2905–2908, 1998.

[12] Krupp, N. et al., Energetic particle bursts in the predawn Jovian magnetotail, Geophys. Res. Lett., Vol.25, pp.1249–1252, 1998.

[13] Kronberg, E. A. et al., A possible intrinsic mechanism for the quasi-periodic dynamics of the Jovian magnetosphere, J. Geophys. Res., Vol.112, doi: 10.1029/2006JA011994, 2007.

[14] Yoneda, M. et al., Brightening event seen in observations of Jupiter's extended sodium nebula, Icarus, Vol.261, pp.31-33, 2015.

[15] Klein, M. J. et al., Changes in Jupiter's 13-cm synchrotron radio emission following the impact of comet Shoemaker-Levy-9, Geophys. Res. Lett., Vol.22, pp. 1797-1800, 1995.

[16] de Pater, I., 21 cm maps of Jupiter's radiation belts from all rotational aspects, Astron. Astrophys., Vol.88, pp. 175–183, 1980.

[17] Kita, H. et al., Effect of solar UV/EUV heating on the intensity and spatial distribution of Jupiter's synchrotron radiation, J. Geophys. Res., Vol.118, doi:10.1002/jgra.50568, 2013.

[18] Clarke, J. T. et al., Response of Jupiter's and Saturn's auroral activity to the solar wind, J. Geophys. Res., Vol.114, doi:10.1029/2008JA013694, 2009.

[19] Kimura, T. et al., Transient internally driven aurora at Jupiter discovered by Hisaki and the Hubble Space Telescope, J. Geophys. Res., Vol.42, doi:10.1002/2015GL063272, 2015.

A Proposal Constructing mm/sub-mm VLBI Network by Japanese/East-Asian Power

Makoto Miyoshi (*makoto.miyoshi@nao.ac.jp*), **T. Kasuga (Hosei Univ.), M. Tsuboi (ISAS), M. Takahashi (Aichi Univ. Edu.), T. Oka, S. Takekawa (Keio Univ.), N. Takato (NAOJ), H. Ujihara (NICT), H. Ishitsuka, V. Erick (IGP, Peru), & the CARAVAN team**

National Astronomical Observatory, Japan, 2-21-1, Osawa, Mitaka, Tokyo, Japan 181-8588

Abstract: We report here the recent progress in CARAVAN-submm and note that a global mm/sub-mm VLBI network can be constructed by collaborations with astronomical institutions in East Asia. East Asia has a potential power promoting next black hole imaging observations.

1. Imaging black holes and CARAVAN-submm

Imaging surroundings of black holes are fascinating observations that mm/sub-mm VLBI can achieve in very near future. For the purpose, Japan has a dedicated plan, "CARAVAN-submm", which is a project constructing a mm/sub-mm VLBI network at Andes. It contains at least two fixed VLBI stations and one mobile VLBI station, which is a famous method in Japanese geodetic VLBI experiments since mid in the 1980s (Ichikawa et al., 2009). Using the same method we sample visibility data from shorter baselines around 1000 $\sim$ 2000 *km at* $230GHz$ effectively and attain higher quality images at submm VLBI observations than those only fixed stations can do. By observing SgrA*, a super massive black hole at our galactic center, we aim imaging observations of the surroundings of the black hole horizon, and pave the way for observing verification of the general relativity and open observational black hole astrophysics (Miyoshi et al., 2011) [1]. Next following sections, we report recent progress of CARAVAN-submm.

2. Observing Site Survey at Andes 2015

We plan to construct the fixed stations at around Huancayo Observatory (3370 m in altitude), IGP in Peru and at the Chacaltaya Cosmic Ray Observatory (5300 m in altitude) in Bolivia. We performed new site survey both in Peru and Bolivia for investigating the precipitable water vapor amounts in 2015. By the infrared water vapor meter used at our previous survey in 2012, we found the precipitable water vapor amounts in the rainy reason

[1]CARAVAN-submm was openly discussed as one of middle class projects in the Astronomy and Astrophysics subcommittee of Science Council of Japan (SCJ) in 2012.

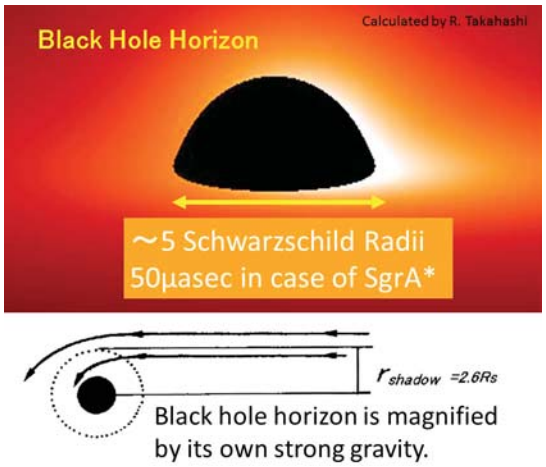

Figure 1. Image of black hole shadow calculated by R. Takahashi (2005). The black hole shadow size in SgrA is about* $50\mu asec$ *in diameter.*

Figure 2. CARAVAN-submm at Andes. The mobile radio telescope CARAVAN-submm moves around Andes. By changing positions of observations, we can obtain VLBI data from various baseline lengths and directions. In the data the null point should be contained, which is the strong evidence of the existence of a black hole horizon in the image. We plan to use multi mirror system for making a light weighted telescope. The CARAVAN-submm will contain at least three of trucks. One for antennas, another for mount, and the other is for electric power-supply and VLBI recording system and hydrogen maser. Though we suppose power supply for operating telescope is commercial base. The Peruvian and Bolivian Andes are the civilized regions. There are many cities and towns. Commercial based electric power supply is easily obtained. Also the main roads are developed along the Andes, therefore the movement of CARAVAN-submm telescope is quite easily preformed.

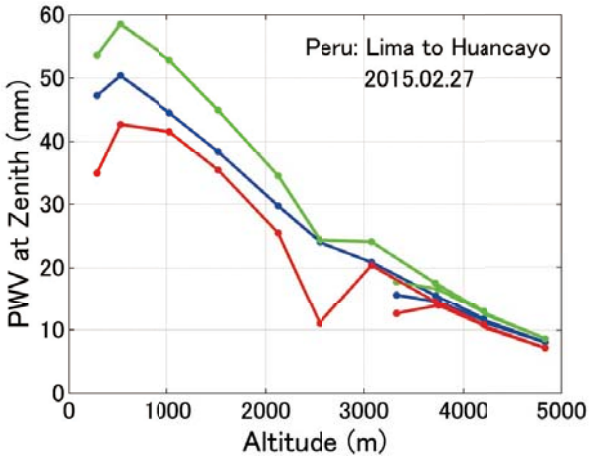

Figure 3. PWV v.s. Altitude along the road from Lima to Huancayo in Peru (2015.2.27). The three color lines show PWVs measured from different absorption lines of water vapor.

(February to March in 2015) were worse at least two times as compared with those in dry seasons. This means that the best seasons for mm/sub-mm VLBI observations are limited even in Andes higher mountains.

3. Cost reduction of high precision antennas

In order to realize the cost reduction in making high precision antennas for receiving millimeter to sub-millimeter wavelength, we have examined the accuracy of the palabra surfaces made by metal spinning method, and found that an accuracy as well as $60\mu m$ *r.m.s.* is easily obtained (Miyoshi et al. 2013). Recently we confirmed that surface accuracies about $15\mu m$ *r.m.s.* were achieved by adding an annealing process between spinning process. Now we have hopeful outlooks that cost reduced mm/sub-mm antennas as large as 2 m in diameter can be produced by using metal spinning method.

4. A Proposal Constructing mm/sub-mm VLBI Network by Japanese/East-Asian Power

Astronomical institutions in East Asia have own good mm/sub-mm radio telescopes, namely JCMT 15m (EAO), ASTE 10m (NAOJ), SPART 10m (Osaka Perf.,& NRO,NAOJ), GLT 12m (ASIAA), and three of 20m radio telescopes in KVN. Also Nobeyama 45m telescope (NRO,NAOJ) can be used for mm/sub-mm VLBI. Adding with a future plan CARAVAN-submm at Andes, astronomical institutions in East Asia have a potential power promoting global mm/sub-mm VLBI observations if they collaborate each other. East Asia has a long history of the black hole study, related future plans, and powerful observing instruments. We have a

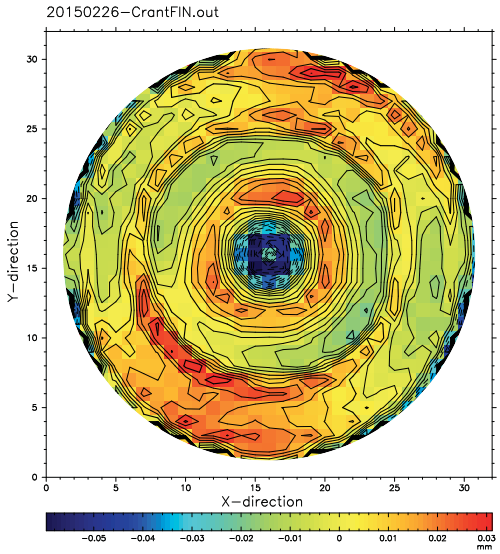

Figure 4. Surface accuracy about $15\mu m$ *r.m.s. was achieved using a new 30 cm mold (surface accuracy:* $4\mu m$ *r.m.s.) by metal spinning method with adding a annealing process.*

chance to construct a global sub-mm VLBI array by East Asian power. East Asia can be the next leading force in the black hole imagings.

Figure 5. JCMT 15 m at Hawaii http://www.eaobservatory.org/jcmt/

References

[1] Miyoshi, M. et al., ,in Proceedings of the 12th NICT TDC Symposium (Kashima, June 6, 2013) , Technical Development Center News, NICT, ISSN 1832-3432, **33**, 15-17, (2013)

[2] Miyoshi, M. et al., A First Black Hole Imager, CARAVAN-sub at Andes, 2011ASPC,439, 279M (2011)

[3] Ichikawa, R., A. et al., IVS NICT-TDC News No.30, (2009)

[4] Takahashi, R., PASJ, 57,273-277, (2005).

First Japanese 230 GHz VLBI experiment by MICE2015 team

Kazuhiro Takefuji (*takefuji@nict.go.jp*)[1] **on behalf of MICE2015 team**

[1] *Kashima Space Technology Center, National Institute of Information and Communications Technology, 893-1 Hirai, Kashima, Ibaraki 314-8501, Japan*

Abstract: We carried out a 230GHz VLBI experiment on 200 m baseline between Solar Planetary Atmosphere Research Telescope(SPART) 10m and 1.85m telescopes in Nobeyama Radio Observatory (NRO) in the end of April 2015. The project name was so-called, MICE2015 (Mm Interferometer Collaboration Experiment 2015, PI: Prof. Fujisawa of Yamaguchi university). We installed VLBI equipment (e.g A/D sampler, recording terminal, stabilized reference signal transfer, and two OCXOs) to each telescope. We observed an edge of the Moon as a strong fringe finder, then successfully we obtained fringes. Here we will report more detail of the experiment and the fringe properties.

1. Introduction

Event Horizon Telescope (EHT) promotes strongly research in obtaining a shadow of the super massive black hole of SgrA∗, M87, and so on by (sub-)mm VLBI [1]. The 200 GHz range VLBI has a 25 years history [3]. However, the highest frequency range of Japanese VLBI recorded still 85 GHz[4]. Based on these situations, MICE2015 team focused on making a first 230 GHz VLBI in Japan with using two telescope in Nobeyama for gaining a mm-VLBI technique and experience.

2. MICE2015: First 230 GHz VLBI

Nobeyama has a long history of Japanese radio astronomy since 1960's establishing 45m telescope, Nobeyama millimeter array (NMA) as prototype ALMA. Nowadays two telescope SPART 10m (In those days called No.F in NMA) and 1.85m on 150m baseline have each 230 GHz cryogenic receiver in NRO. However both antennas have no VLBI equipment, thus VLBI backends including digital sampler and recorder and stabilized reference signal transfer system were installed after brought by authors.

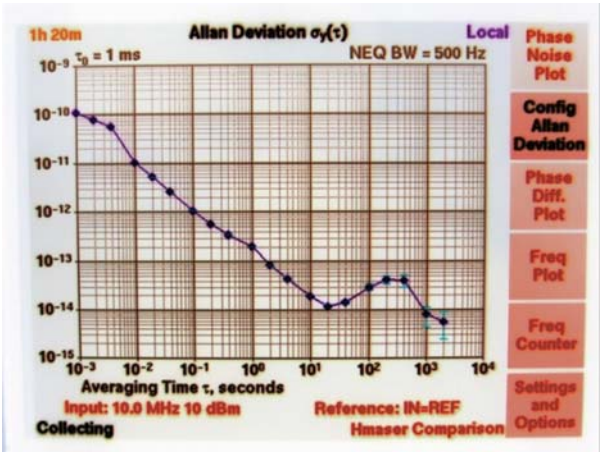

Figure 1. Stabilized reference transfer measurement before shipping. The result of Alan standard deviation shows $1 * 10^{-14}$ *in 1sec integration.*

2.1 Installation of VLBI equipment

At first we laid a 200 meter optical-fiber between 13m antenna and 1.85m antenna and installed stabilized reference signal transfer system for just finding fringe as a first step. Table. 1 shows their specification. Before installing, we measured its stability with DMTD in NICT/Kashima. Figure 1 shows a result of closed loop measurement between its transmitter and receiver. Since the result of Alan standard deviation shows $1 * 10^{-14}$ stability in 1 sec integration, it seems to be sufficient ($2.3 * 10^{11}[Hz] * 1 * 10^{-14} = 2.3 * 10^{-3}$) for 230 GHz VLBI. We also installed OCXO reference and GPS for positioning and generating 1PPS signal to each antenna. Down-converted IF signal from DC to 1GHz range of each antenna was connected to digital sampler (K6/GALAS), which can sample 16GHz speed. Then, 1GHz bandwidth can be recorded with DBBC functions of the K6/Galas.

2.2 VLBI on the Moon edge

Such high frequency, bright sources for detecting VLBI are not so many. But the edge of the Moon would be a good candidate [5, see Appendix 10.1]. First we connected stabilized reference 10 MHz signal, which we transfers from SPART 10m to 1.85m. Then, we observed the Moon for 1 minutes. Just after recording, we performed a correlation immediately with software correlator GICO3 developed by NICT. We might have a luck, we could successfully detect fringe (figure 2). We see 4 Hz residual in rate. This is a predicted rate, whose difference caused by SPART 10m down-converter setting. Af-

Name	SPART	OPU1.85
Diameter [m]	10	1.85
Pol	Linear	Circular
Tsys[K]	—	200
X[m]	-3871061.02	-3871175
Y[m]	3428327.24	3428279
Z[m]	3723784.271	3723701

Table 1. A specification of each antenna. The XYZ position were determined roughly by google map (their longitude and latitude) and GPS (height). A setting polarization of SPART 10m was initially circular, but it was changed to linear pol for detecting fringe.

ter we obtained fringe, we changed reference signal of both antennas to OCXO reference, which has quite high stability developed by JAXA and NAOJ. We successfully obtained real VLBI (not so long baseline) fringe with rate tuning after the replacement of reference signal (see figure 3).

3. Discussion: A coherence computed by 230 GHz fringe

Greve et.al reported that the coherence times were the order of 10 sec., most probably limited by the atmosphere in their 215 GHz VLBI [2]. If we make a 230 GHz VLBI through the the atmosphere with stability in the order of 10^{-13}, the time interval to change the phase about 1 cycle will be only about 43 sec $= 1/(230 * 10^9 * 10^{-13})$. Before we exchange the reference signal source to OCXO, we observed the Moon for 1 hour. Figure 4 shows residual rate before (red) and after (green line) fine tuning of clock model ($\dot{\tau}, \ddot{\tau}, \dddot{\tau}$ determined by data) in an a priori file for correlation. We could almost compensate the rate variation. However the 230 GHz fringe phase had still quadric curvature, then we removed it by quadric fitting. Finally the residual phase was converted to delay as a time series. Figure 5 shows the residual delay which includes +1 to -1 ps variation. Then we perform noise analysis by Fourier transform the figure 5. The result of Fourier analysis is shown in figure 6. The figure has the bending point around 400 sec, as a coherent time. It indicates that white noise component is dominated from 10 sec to 400 sec, but flicker noise component becomes predominant after 400 sec in case we could remove the quadratic phase change. If the coherence time of '400 sec.'

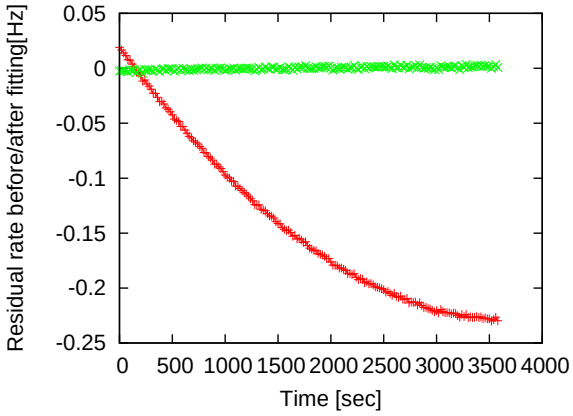

Figure 4. Fine tuned residual rate (green) and initial result (red).

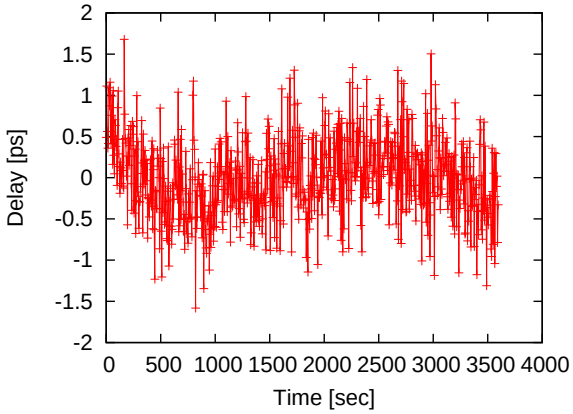

Figure 5. A residual delay after fine tuned with clock model and quadric fitting.

appeared only for the case of stabilized reference signal, it has almost a good agreement in DMTD result $434[sec] = 1/(230 * 10^9 * 10^{-14}))$(figure. 1). This experiments were a just first step, we would like to make longer baseline VLBI in future.

Acknowledgements

All Japan VLBI researcher was cooperated to MICE2015, which includes Yamaguchi univ, Osaka Pref univ, Ibaraki univ, NAOJ, JAXA/ISAS, NAO, Kyoto univ and NICT/Kashima. The author thanks everyone for supporting the experiment and cooperation.

References

[1] S. S. Doeleman, J. Weintroub, A. E. E. Rogers, R. Plambeck, R. Freund, R. P. J. Tilanus, P. Friberg, L. M. Ziurys, J. M. Moran, B. Corey, K. H. Young, D. L. Smythe, M. Titus,

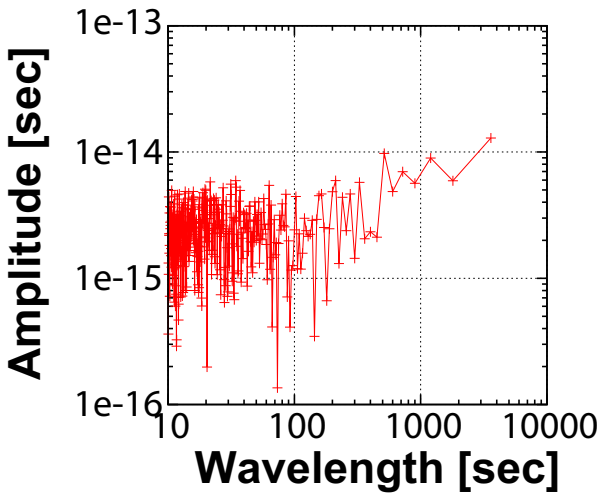

Figure 6. Power spectrum of the figure 5. We can see bending point at near 400 sec.

D. P. Marrone, R. J. Cappallo, D. C.-J. Bock, G. C. Bower, R. Chamberlin, G. R. Davis, T. P. Krichbaum, J. Lamb, H. Maness, A. E. Niell, A. Roy, P. Strittmatter, D. Werthimer, A. R. Whitney, and D. Woody. Event-horizon-scale structure in the supermassive black hole candidate at the Galactic Centre. *Nature*, 455:78–80, September 2008.

[2] A. Greve, M. Torres, J. E. Wink, M. Grewing, W. Wild, J. Alcolea, A. Barcia, F. Colomer, P. de Vincente, J. Gomez-Gonzalez, I. Lopez-Fernandez, D. A. Graham, T. P. Krichbaum, R. Schwartz, K. J. Standke, A. Witzel, and A. Baudry. 215 GHz VLBI observations: Detection of fringes on the 1147 KM baseline Pico Veleta-Plateau de Bure. *A&A*, 299:L33, July 1995.

[3] S. Padin, D. P. Woody, M. W. Hodges, A. E. E. Rogers, D. T. Emerson, P. R. Jewell, J. Lamb, A. Perfetto, and M. C. H. Wright. 223 GHz VLBI observations of 3C 273. *ApJ letter*, 360:L11–L13, September 1990.

[4] K. M. Shibata, H.-S. Chung, S. Kameno, D.-G. Roh, T. Umemoto, K.-D. Kim, K. Asada, S.-T. Han, N. Mochizuki, S.-H. Cho, S. Sawada-Satoh, H.-G. Kim, T. Bushimata, Y. C. Minh, T. Miyaji, N. Kuno, H. Mikoshiba, K. Sunada, M. Inoue, and H. Kobayashi. First mm-VLBI Observations between the TRAO 14-m and the NRO 45-m Telescopes: Observations of 86 GHz SiO Masers in VY Canis Majoris. *PASJ*, 56:475–480, June 2004.

[5] A.R. Thompson, J.M. Moran, and G.W. Swenson. *Interferometry and Synthesis in Radio Astronomy*. Wiley, 2008.

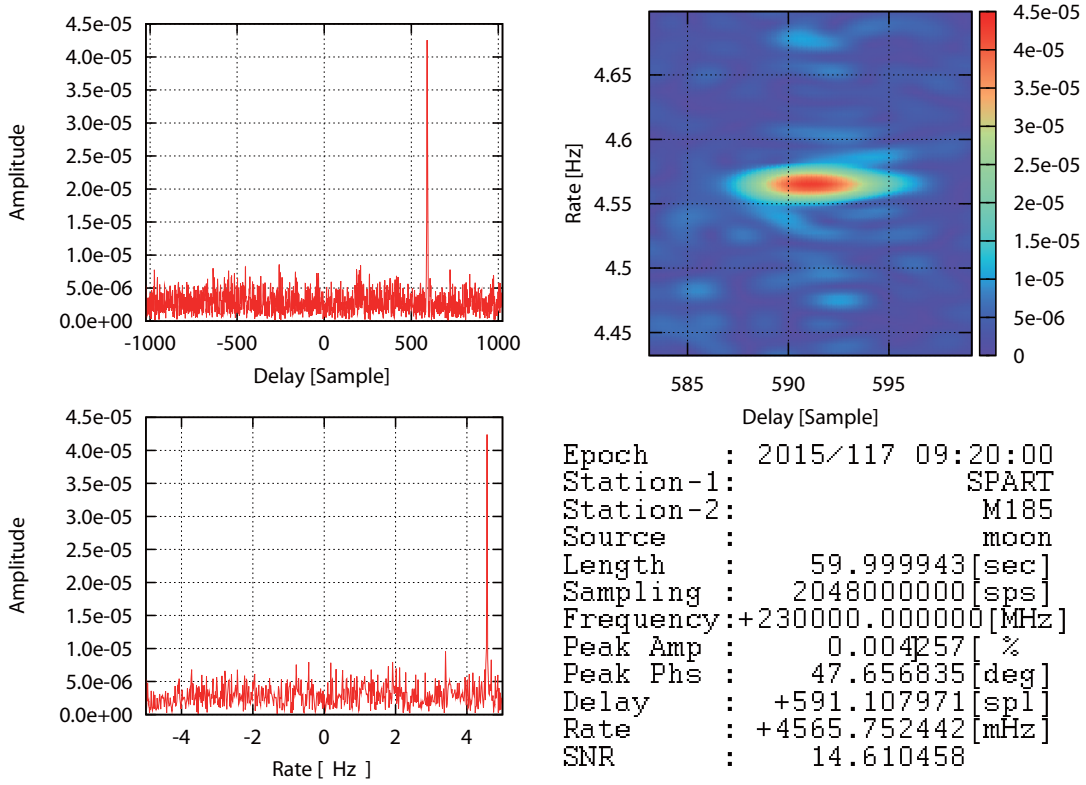

Figure 2. The first 230GHz fringe of Moon edge with common reference signal.

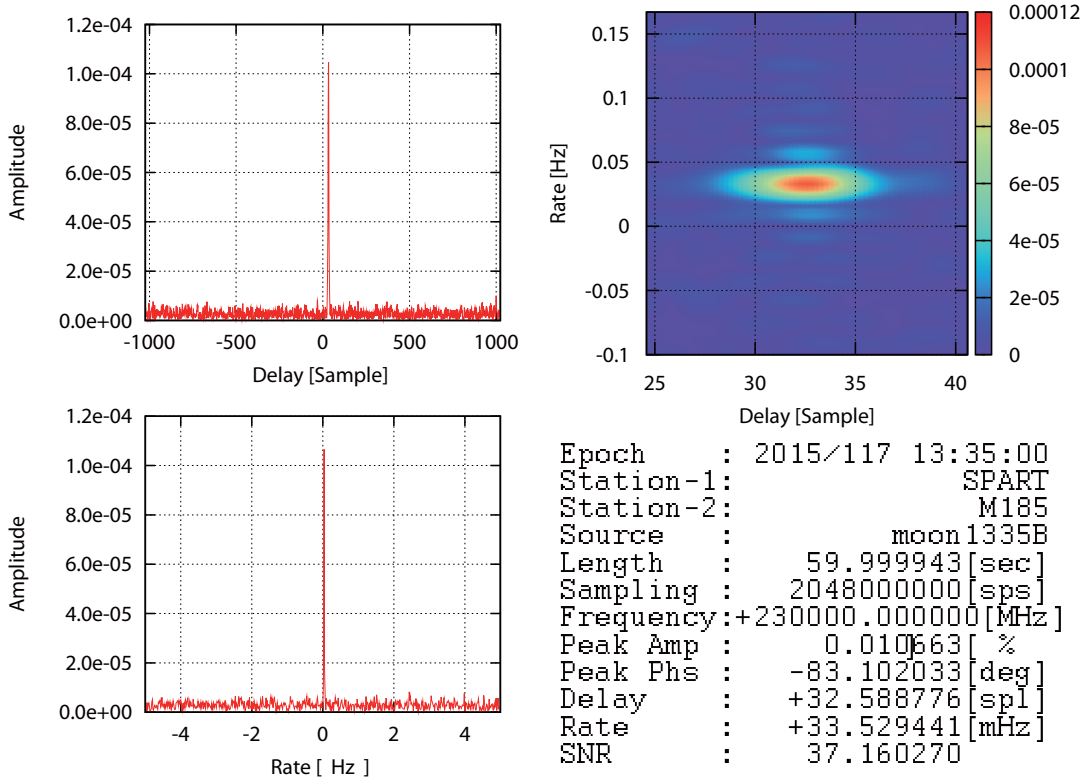

Figure 3. The first 230GHz VLBI fringe of Moon edge with independent reference signal of OCXO.

"IVS NICT Technology Development Center News" (IVS NICT-TDC News) published by the National Institute of Information and Communications Technology (NICT) (former the Communications Research Laboratory (CRL)) is the continuation of "IVS CRL Technology Development Center News" (IVS CRL-TDC News). (On April 1, 2004, Communications Research Laboratory (CRL) and Telecommunications Advancement Organization of JAPAN (TAO) were reorganized as "National Institute of Information and Communications Technology (NICT)".)

VLBI Technology Development Center (TDC) at NICT is supposed

1) to develop new observation techniques and new systems for advanced Earth's rotation observations by VLBI and other space techniques,
2) to promote research in Earth rotation using VLBI,
3) to distribute new VLBI technology,
4) to contribute the standardization of VLBI interface, and
5) to deploy the real-time VLBI technique.

The NICT TDC newsletter (IVS NICT-TDC News) is published biannually by NICT.

This news was edited by Mamoru SEKIDO, Kashima Space Technology Center. Inquires on this issue should be addressed to Mamoru SEKIDO, Kashima Space Technology Center, National Institute of Information and Communications Technology, 893-1 Hirai, Kashima, Ibaraki 314-8501, Japan, e-mail : sekido@nict.go.jp.

Summaries of VLBI and related activities at the National Institute of Information and Communications Technology are on the Web. The URL to view the home page of the Radio Astronomy Applications Section of the Space-Time Measurement Group of Space-Time Standards Laboratory is : **"http://www2.nict.go.jp/aeri/sts/stmg/index_e.html"**.

IVS NICT TECHNOLOGY DEVELOPMENT CENTER NEWS No.35, October 2015

International VLBI Service for Geodesy and Astrometry
NICT Technology Development Center News
published by
National Institute of Information and Communications Technology, 4-2-1 Nukui-kita, Koganei, Tokyo 184-8795, Japan